Bridging Born and Lindemann criteria: The role of interstitial defects

Yajun Zhou* and Xiaofeng Jin†
Surface Physics Laboratory & Department of Physics, Fudan University, Shanghai 200433, China
(Received 25 January 2005; revised manuscript received 22 February 2005; published 27 June 2005)

We investigate theoretically the crucial role of the interstitial defects that trigger the melting of a surface-free elemental crystal. Based on a modified J_1-J_2 lattice model, we have studied the quasistatic and dynamic properties of a face-centered-cubic elemental crystal. The avalanche of interstitial defects due to cooperation proves to be the instability mechanism at the melting point that bridges Lindemann and Born criteria.

DOI: 10.1103/PhysRevB.71.224113 PACS number(s): 64.60.Cn, 64.70.−p

I. INTRODUCTION

Bulk melting is a solid-liquid phase transition (SLPT) taking place in a surface-free crystal.[1] The study of this phenomenon helps to clarify the essential driving force of the inhomogeneous phase transition out of a homogeneous system in that the surface-free condition rules out the influence of inhomogeneity at the surface boundary. Many endeavors have been made to test the previous melting theories by probing into the behavior of bulk melting,[2] especially in search of the relation between the widely cited Lindemann[3] and Born[4] criteria. The Lindemann criterion proposes that melting is triggered by the avalanche of the root-mean-square (rms) atom displacement after it exceeds a threshold fraction (δ_L^*) of the atom spacing (a), where δ_L^* is called the critical Lindemann ratio, a semiempirical parameter once conceived as a lattice type characteristic; the Born criterion argues that the vanishing of the shear modulus is responsible for the inability to resist lattice destruction at the melting point.

Nevertheless, in one recent molecular dynamics simulation, Jin *et al.*[5] used numerical results to demonstrate that a surface-free argon (Ar) crystal undergoes a first-order SLPT when the shear moduli experience a sudden downfall (albeit not exactly vanishing, which is consistent with the experimental observation of residual shear modulus at the melting point[6]) and the atom displacement surges to infinity simultaneously. In this visualization of the agreement of the Lindemann and Born criteria, Jin *et al.* attributed the agreement at the superheating limit (namely, the "melting point" of a surface-free crystal, referred to as T_m hereafter) to the observation that "Lindemann particles" (the atoms whose rms displacement exceeds $a\delta_L^*$) tend to aggregate as a "liquid nucleus" and the atoms in this nucleus manifest nearly vanishing shear modulus difference $\Delta C_S = C_{44} - (C_{11} - C_{12})/2 \approx 0$.[5] In other words, each cluster of Lindemann particles satisfies both criteria, and the expansion of these clusters marks the steady growth of a liquid phase. The numerical results in Ref. 5 have implications for several important questions whose answers remain elusive.

Question 1. Are there any parameters of the interatomic forces that may account for the magnitude of the parameter δ_L^*, which seems to vary from crystal to crystal?[7]

Question 2. What kind of instability mechanism is directly responsible for the nonzero shear moduli at T_m, which seems to contradict Born's original argument?

Question 3. How does a heterogeneous nucleation process manage to come out from a homogeneous system, that is, how does a surface-free solid generate an interface from within?

The answers to these three questions will definitely improve our understanding of superheating, an important process in thermodynamics[8] that is experimentally realizable by either material coating[1] or laser-induced local heating.[9]

In this paper, we report an analytical procedure to join the Lindemann and Born criteria in the case of bulk melting—the SLPT in a boundary-free system as studied in Ref. 5, and address the three numbered queries above. In Sec. II, following the idea of defect-motivated transition in previous literature[10–13] and the previous understanding of defect cooperation and aggregation,[11,14–21] we use the J_1-J_2 lattice model plus a vibrational Hamiltonian[22] to formulate the motion of atoms in a solid, and show that in terms of the mean-field approximation (MFA) and variational method, the model manifests a first-order phase transition. Section III discusses the physical implications that underlie the model solutions, including the symmetry of the Hamiltonian, a chemical equilibrium analogy, and the origin of "Lindemann particles." Section IV interprets the coincidence of Born and Lindemann criteria in the light of the model solution and answers the three aforementioned questions intractable using numerical results.

II. MODEL HAMILTONIAN AND PHASE TRANSITION

A. Total Hamiltonian

We begin our argument with the Hamiltonian for a system of $N=4\ell^3$ atoms, labeled as $\alpha=1,\ldots,N$:

$$\mathcal{H} = \sum_{\alpha=1}^{N}\left(T_\alpha + \frac{1}{2}\sum_{\beta=1}^{N} V_{\alpha\beta}^{\mathrm{vib}}\right) + \frac{1}{2}\sum_{\alpha=1}^{N}\sum_{\beta=1}^{N} V_{\alpha\beta}^{\mathrm{conf}}. \qquad (1)$$

This Hamiltonian incorporates the kinetic energy of each atom labeled α (T_α) and pairwise potential energy between atoms α and β ($V_{\alpha\beta}=V_{\alpha\beta}^{\mathrm{vib}}+V_{\alpha\beta}^{\mathrm{conf}}$), where $V_{\alpha\alpha}=0$, for $\alpha=1,\ldots,N$. For each atom labeled α, the potential energy that it experiences reads $\Sigma_{\beta=1}^{N} V_{\alpha\beta}$, which finally breaks down to the summation of the "vibrational potential" $\Sigma_{\beta=1}^{N} V_{\alpha\beta}^{\mathrm{vib}}$ and the "configurational potential" $\Sigma_{\beta=1}^{N} V_{\alpha\beta}^{\mathrm{conf}}$. The former is harmonically oscillating with respect to interatomic distance when the atom α is *perturbed*, and the latter is formally defined as

$\Sigma_{\beta=1}^{N}(V_{\alpha\beta}-V_{\alpha\beta}^{\mathrm{vib}})$. This method of separating the Hamiltonian was once successfully employed to explore the extent to which lattice vibration affects the concentration of crystal defects.[22]

This work basically treats an elemental crystal with face-centered-cubic (fcc) structure (Ar, for instance). In order to take the interstitial defects into account, we use a lattice model with the standard NaCl-type structure. At absolute zero, the Na-like lattice is totally occupied by Ar atoms, while the Cl-like lattice is vacant and forms the totality of octahedral holes in a perfect fcc crystal. At any finite temperature, by disregarding the vibrations and lattice distortions (that is, by neglecting the atoms' kinetic energy and its consequences) for the moment, one may caricature the motion of the atoms in the solid by stochastic hops on the two interpenetrating fcc lattices. The configurations of the system are thus exhausted by all the possible ways to arrange N atoms of a fcc crystal at $2N$ possible sites, so the summation over atom pairs can be converted to a summation over site pairs, as long as the site occupancy rate n at position $\mathbf{r}=(hkl)$ is included in the following way:

$$\frac{1}{2}\sum_{\alpha=1}^{N}\sum_{\beta=1}^{N}V_{\alpha\beta}^{\mathrm{conf}}=\frac{1}{2}\sum_{\mathbf{r}}\sum_{\mathbf{r}'}J_{\mathbf{r}\mathbf{r}'}^{\mathrm{conf}}n_{\mathbf{r}}n_{\mathbf{r}'}\approx\frac{1}{2}\sum_{h,k,l=1}^{2\ell}n_{hkl}\left(J_1\sum_{h'k'l'}n_{h'k'l'}+J_2\sum_{h''k''l''}n_{h''k''l''}\right). \tag{2}$$

Here, $\Sigma_{\mathbf{r}}$ denotes summation over all the $2N$ sites, $|h-h'|+|k-k'|+|l-l'|=1$, $|h-h''|+|k-k''|+|l-l''|=2$, and $n_{\mathbf{r}}$ denotes the number of the atoms occupying the site at position $\mathbf{r}$, $n_{\mathbf{r}}=0$ or 1. We have the cyclic boundary condition $n_{h+2\ell,k,l}=n_{h,k+2\ell,l}=n_{h,k,l+2\ell}=n_{h,k,l}$ which eliminates the surface boundary; and the atom number conservation condition $\Sigma_{h,k,l=1}^{2\ell}n_{hkl}=N$ which reduces the degree of independence for the occupancy rate by 1. The "coupling constant" $J_{\mathbf{r}\mathbf{r}'}^{\mathrm{conf}}$ equals $V_{\alpha\beta}^{\mathrm{conf}}$ when the distance between two atoms α and β is equal to $|\mathbf{r}-\mathbf{r}'|$. We have used the following cutoff in Eq. (2): $J_{\mathbf{r}\mathbf{r}'}^{\mathrm{conf}}=J_1$ when $|\mathbf{r}-\mathbf{r}'|$ is the nearest-neighbor (NN) distance, namely, the distance between a pair of nearest "Na" and "Cl;" $J_{\mathbf{r}\mathbf{r}'}^{\mathrm{conf}}=J_2<0$ when $|\mathbf{r}-\mathbf{r}'|$ is the next-nearest-neighbor (NNN) distance, namely, the distance between a pair of nearest "Na" sites (or "Cl" sites); $J_{\mathbf{r}\mathbf{r}'}^{\mathrm{conf}}=0$ otherwise. In order that the NNN distance becomes the bond length in the fcc crystal in our model (such as Ar, as opposed to NaCl), we require that $J_1>J_2$ and $J_2<0$. This J_1-J_2 lattice model approximation is justified for interatomic forces that are both pairwise and short ranged, which is physically applicable to solids where the interaction is governed by the Lennard-Jones (as in noble gases) or Morse functions (as in some metals).[21]

In the three-dimensional lattice, vibrations are taken into consideration in the form of the vibrational free energy

$$F^{\mathrm{vib}}=3Nk_BT\ln\frac{h\nu}{k_BT}, \tag{3}$$

where k_B is the Boltzmann constant, T is the absolute temperature, h is the Planck constant, and ν is the geometric mean frequency of the vibrations.[22,23] The formula above is valid in the Dulong-Petit limit—the temperature regime where most melting processes take place and the heat capacity contributed by lattice vibration is asymptotically $3Nk_B$.

B. Mean-field approximation

According to Landau-Ginzburg theory,[24] the free-energy functional related to Eq. (2) has the expansion

$$F^{\mathrm{conf}}[L(\mathbf{r})]=\frac{1}{\sqrt{2}a^3}\int d^3\mathbf{r}\left\{[1-L^2(\mathbf{r})]\mathcal{H}_1+[1-L^2(\mathbf{r})]^2\mathcal{H}_2+\gamma[\nabla L(\mathbf{r})]^2+6J_2+k_BT\left(\ln\frac{1-L^2(\mathbf{r})}{4}+L(\mathbf{r})\ln\frac{1+L(\mathbf{r})}{1-L(\mathbf{r})}\right)\right\} \tag{4}$$

where $L(\mathbf{r})=\langle(-1)^{h+k+l}(2n_{hkl}-1)\rangle$ is a local order parameter. Here, $\langle\cdot\rangle$ denotes the ensemble average—the weighted average over all configurations that the system is able to sample through. Within a region where $L(\mathbf{r})>0(<0)$, atoms preferentially occupy even (odd) $h+k+l$ sites. The $T=0$ K ground state is then described by either $L(hkl)\equiv+1$ or $L(hkl)\equiv-1$. $\mathcal{H}_1\doteq(3/2)(-2J_2+J_1)>0$ evaluates the excitation energy of isolated interstitial defects, and $\mathcal{H}_2\doteq(3/8)J_2<0$ denotes the energy trade-off to excite two interstitial defects at NNN distance instead of farther apart (i.e., "virtual attraction between defects"[11]), $\gamma\doteq a^2\mathcal{H}_1/2$ is the domain-wall energy coefficient, where a is the average atom spacing. Here, "$\doteq$" denotes some crude estimates based on the MFA, as illustrated later by some "graph counting" of interactions between neighboring sites. The logarithmic terms in the integrand of $F^{\mathrm{conf}}[L(\mathbf{r})]$ result from the configurational entropy S^{conf}.[25]

The kinetic energy and the vibrational potential in the original Hamiltonian in Eq. (1) boil down to the vibrational free-energy functional $F^{\mathrm{vib}}[L(\mathbf{r})]=-(3k_BT/\sqrt{2}a^3)\int d^3\mathbf{r}[1-L^2(\mathbf{r})]\Upsilon$. Here, $\Upsilon=(1/4)\ln(\nu_l/\nu_i)>0$ where subscripts i and l refer to (the vibrational modes at) the interstitial sites and the lattice sites, respectively. This logarithmic term, which is a consequence of Eq. (3), agrees with the lattice model modified by different eigenfrequencies of vibration in Ref. 22.

The representation of $\mathcal{H}_1$ and $\mathcal{H}_2$ in terms of J_1 and J_2 can be done by assuming a uniform $L(\mathbf{r})$ and rewriting

$$F^{\mathrm{conf}}+TS^{\mathrm{conf}}=\sum_{\mathbf{r}}(6J_1\langle n_{\mathbf{r}}n_{\mathbf{r}'}\rangle+12J_2\langle n_{\mathbf{r}}n_{\mathbf{r}''}\rangle)=\sum_{\mathbf{r}}[6J_2+[1-L^2(\mathbf{r})]\mathcal{H}_1+[1-L^2(\mathbf{r})]^2\mathcal{H}_2], \tag{5}$$

and using the approximation

$$\langle n_{\mathbf{r}}n_{\mathbf{r}'}\rangle\doteq\langle n_{\mathbf{r}}\rangle\langle n_{\mathbf{r}'}\rangle=\frac{1+|L(\mathbf{r})|}{2}\frac{1-|L(\mathbf{r})|}{2}=\frac{1-L^2(\mathbf{r})}{4}, \tag{6}$$

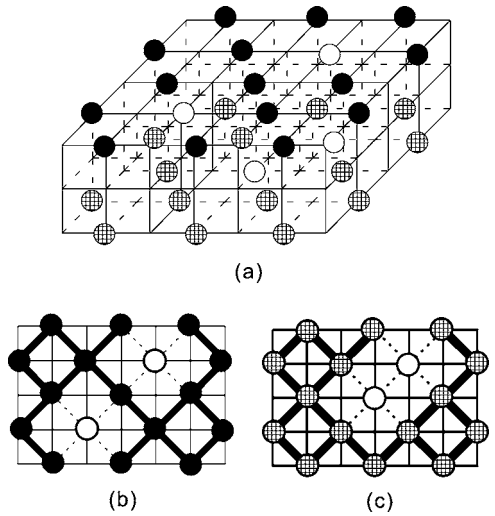

FIG. 1. (a) This shows two layers in a crystal. In the "upper layer" (atoms represented by filled circles), the two holes are separate whereas in the "lower layer" (checkered circles), the two holes are close. (b) This shows the cross-section view of the upper layer, with loss of eight bonds (in dashed lines) as compared to a perfect layer. (c) This shows the cross-section view of the lower layer, with loss of seven bonds (in dashed lines) as compared to a perfect layer. We can see that two close holes save bonding energy in the amount of J_2 [bonds are denoted by thick black lines in (b) and (c)].

$$\begin{aligned}\langle n_{\mathbf{r}} n_{\mathbf{r}''}\rangle &= \frac{1}{2}(\langle n_{\mathbf{r}} n_{\mathbf{r}''}\rangle_l + \langle n_{\mathbf{r}} n_{\mathbf{r}''}\rangle_i)\\ &\doteq \frac{1}{2}(\langle n_{\mathbf{r}}\rangle_l \langle n_{\mathbf{r}''}\rangle_l + \langle n_{\mathbf{r}}\rangle_i \langle n_{\mathbf{r}''}\rangle_i) + g(L(\mathbf{r}))\\ &= \frac{1}{2}\left[\left(\frac{1+|L(\mathbf{r})|}{2}\right)^2 + \left(\frac{1-|L(\mathbf{r})|}{2}\right)^2\right]\\ &\quad + \frac{12}{2}\left(\frac{1-|L(\mathbf{r})|}{2}\right)^2\\ &= \frac{1}{2} - \frac{1-L^2(\mathbf{r})}{4} + \frac{3}{8}[1-L^2(\mathbf{r})]^2. \end{aligned} \tag{7}$$

Here, $g(L(\mathbf{r}))$ is an estimate of the correction due to the NNN correlation, assuming that the system saves the binding energy in the amount of J_2 when two holes on the lattice sites are close (in NNN contact) instead of being farther apart (see Fig. 1). In total, the saved bonds (NNN interactions) by stochastic contact of holes lower the system energy in the amount of $(3/8)|J_2|[1-L^2(\mathbf{r})]^2$. Physically speaking, $[1-L^2(\mathbf{r})]\mathcal{H}_1$ evaluates the energy cost to excite interstitial defects to be the creation of six antibonds (NN interaction) and annihilation of 12 bonds; $[1-L^2(\mathbf{r})]^2\mathcal{H}_2$ offsets the overestimate in the bond annihilation due to the cooperative excitation of interstitial defects at NNN distance—a non-negligible process when the concentration of interstitial defects exceeds the level of 3%–5%.

The domain-wall energy $\gamma[\nabla L(\mathbf{r})]^2$ is offsetting the miscalculation (Δ) based on the "mean-field" assumption $L(\mathbf{r}) = L(\mathbf{r}') = L(\mathbf{r}'')$ when spatial inhomogeneity is significant:

$$\begin{aligned}&\Delta(2J_1\langle(2n_{\mathbf{r}}-1)(2n_{\mathbf{r}'}-1)\rangle)\\ &= 2\begin{pmatrix} J_1 \\ p \text{ — } r \\ L(\mathbf{r}) \quad L(\mathbf{r}')\end{pmatrix} - \begin{pmatrix} J_1 \\ p \text{ — } p \\ L(\mathbf{r}) \quad L(\mathbf{r}')\end{pmatrix} - \begin{pmatrix} J_1 \\ r \text{ — } r \\ L(\mathbf{r}) \quad L(\mathbf{r}')\end{pmatrix}\\ &= -J_1(2pr - p^2 - r^2)\\ &= J_1(p-r)^2 = J_1\frac{a^2}{2}[\nabla L(\mathbf{r})]^2. \end{aligned} \tag{8}$$

$$\begin{aligned}&\Delta(2J_2\langle(2n_{\mathbf{r}}-1)(2n_{\mathbf{r}''}-1)\rangle)\\ &= 2\begin{pmatrix} & L(\mathbf{r}'') \\ J_2 & \diagdown\, r \\ p & L(\mathbf{r})\end{pmatrix} - \begin{pmatrix} & L(\mathbf{r}'') \\ J_2 & \diagdown\, p \\ p & L(\mathbf{r})\end{pmatrix} - \begin{pmatrix} & L(\mathbf{r}'') \\ J_2 & \diagdown\, r \\ r & L(\mathbf{r})\end{pmatrix}\\ &= -J_2a^2[\nabla L(\mathbf{r})]^2. \end{aligned} \tag{9}$$

According to the Pythagorean theorem applied to the vector decomposition of $\nabla L(\mathbf{r})$, the total the domain-wall energy contributed by the nonvanishing $\nabla L(\mathbf{r})$ at site $\mathbf{r}$ is thus

$$\frac{1}{4}\times 6\times\frac{1}{2}\left(J_1\frac{a^2}{2} - J_2a^2\right)[\nabla L(\mathbf{r})]^2 = \frac{a^2}{2}\mathcal{H}_1[\nabla L(\mathbf{r})]^2. \tag{10}$$

C. Variational approach and phase transition

By applying the Euler-Lagrange equation to $F^{\text{vib}}[L(\mathbf{r})] + F^{\text{conf}}[L(\mathbf{r})]$, and employing the boundary-free condition, we establish the "Poisson equation"[27]

$$\begin{aligned}\rho(L(\mathbf{r})) \equiv \mathcal{H}_1 L(\mathbf{r}) - 2\mathcal{H}_2 L(\mathbf{r})[L^2(\mathbf{r}) - 1] - 3k_BTL(\mathbf{r})\Upsilon\\ - k_BT\tanh^{-1}L(\mathbf{r}) = -\gamma\nabla^2 L(\mathbf{r}).\end{aligned} \tag{11}$$

The solution to this equation optimizes the free-energy functional $F[L(\mathbf{r})]$ according to the variational method.

The "phenomenological electric charge density" $\rho(L(\mathbf{r}))$ immediately gives rise to a simple mathematical model of the catastrophe of the long-range order: For sufficiently low temperature T, the curve $\rho(L(\mathbf{r}))$ intersects the positive $L(\mathbf{r})$

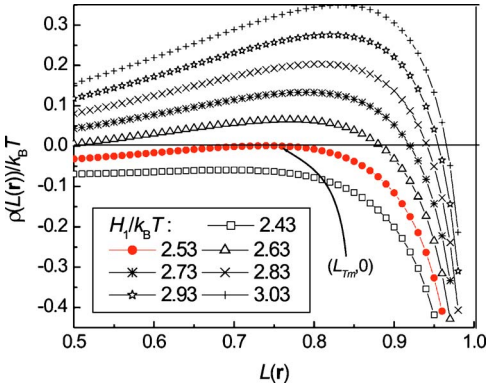

FIG. 2. (Color online) Local properties of $\rho(L(\mathbf{r}))/k_BT$ near its node L_T. Here $\mathcal{H}_1 = 6|\mathcal{H}_2|$, $\Upsilon = \ln(4/3)$. The tangent node is $(L_{T_m}, 0)$.

axis at least once (Fig. 2), so there is a homogeneous distribution $L(\mathbf{r}) \equiv L_T \neq 0$ which makes $\rho(L(\mathbf{r}))$ vanish.[26] Applying

$$\rho(L_{T_m}) = 0 \text{ and } \left.\frac{\partial \rho(L(\mathbf{r}))}{\partial L(\mathbf{r})}\right|_{L(\mathbf{r})=L_{T_m}} = 0$$

to Eq. (11), we can find a threshold temperature T_m satisfying

$$\begin{cases} 3\Upsilon + \dfrac{1}{1-L_{T_m}^2} = \dfrac{\mathcal{H}_1 - 2\mathcal{H}_2(3L_{T_m}^2 - 1)}{k_B T_m}, \\ \dfrac{1}{L_{T_m}^3}\left(\dfrac{L_{T_m}}{1-L_{T_m}^2} - \tanh^{-1} L_{T_m}\right) = -\dfrac{4\mathcal{H}_2}{k_B T_m}, \end{cases} \tag{12}$$

so that the intersection becomes a tangent point when $T = T_m$. The critical order parameter L_{T_m} can be eliminated from the associated equation. (In Fig. 2, $k_B T_m = \mathcal{H}_1/2.53$.) For temperatures higher than T_m, $\rho(L(\mathbf{r}))$ no longer intersects the positive $L(\mathbf{r})$ axis, suggesting a sudden loss of long-range order at T_m, which is typical of a first-order SLPT. As $\mathcal{H}_2$ tends to zero, so does L_{T_m}. Therefore, in the absence of "virtual attraction between defects" (proportional to $\mathcal{H}_2$), a first-order SLPT is not possible according to this model.[28]

Equation (12), the formula pertaining to T_m, physically makes sense in at least two respects.

(1) Every "J_1-J_2 solid" according to our model should bulk melt at a finite temperature

$$T_m = \frac{3|J_2|L_{T_m}^3}{2k_B[L_{T_m}/(1-L_{T_m}^2) - \tanh^{-1} L_{T_m}]} < \frac{9|J_2|}{4k_B} < +\infty, \tag{13}$$

which results from the naive inequality

$$\frac{\lambda}{1-\lambda^2} - \tanh^{-1}\lambda - \frac{2}{3}\lambda^3 = \int_0^\lambda \frac{2x^4(2-x^2)dx}{(1-x^2)^2} > 0 \tag{14}$$

that holds for $0 < \lambda \equiv L_{T_m} < 1$.

In general, Table I justifies the inequality $T_m < 9|J_2|/4k_B$, and shows similar ΔS_{fus} For the noble gases Ne, Ar, Kr, Xe, and Rn, the interaction mode is the well-known van der Waals force and is described by the Lennard-Jones function,[5] so they share theoretically the same (and practically similar) dimensionless parameters $|\mathcal{H}_2|/|\mathcal{H}_1|$, Υ, in our model. Hence they should have almost the same dimensionless values $|L_{T_m}|$, $|J_2|/k_B T_m$, and $\Delta S_{\text{fus}}/N_A k_B$.

(2) For fixed bonding energy J_2 and lattice softening Υ, T_m is lowered when the $|\mathcal{H}_2|/|\mathcal{H}_1|$ ratio is enhanced. This reasonably suggests that the lower the energy cost in excitation of interstitial defects, the lower is the bulk melting point.

The statement above can be translated into

$$\left(\frac{\partial T_m}{\partial \mathcal{H}_1}\right)_{\mathcal{H}_2,\Upsilon} > 0 \tag{15}$$

which is a corollary of the trivial algebra

$$\frac{\partial}{\partial\lambda}\left(\frac{\mathcal{H}_1 - 3k_B T_m \Upsilon}{|\mathcal{H}_2|}\right) = -\frac{4\lambda(1-\lambda^2)^2 \tanh^{-1}\lambda}{[\lambda - (1-\lambda^2)\tanh^{-1}\lambda]^2}\int_0^\lambda \frac{8x^4 dx}{(1-x^2)^3} < 0 \tag{16}$$

and the following argument:

$$\left.\begin{matrix} |\mathcal{H}_2| \text{ is fixed} \\ T_m \nearrow \end{matrix}\right\} \overset{\text{Eq. (12)}}{\Rightarrow} 0 < \lambda = L_{T_m} \searrow \overset{\text{Eq. (16)}}{\left.\begin{matrix} \Rightarrow \mathcal{H}_1 - 3k_B T \Upsilon \nearrow \\ |\Upsilon| \text{ is fixed}, T_m \nearrow \end{matrix}\right\}} \Rightarrow \mathcal{H}_1 \nearrow . \tag{17}$$

III. PHYSICAL IMPLICATIONS OF THE MODEL

A. Symmetry analysis of the configurational Hamiltonian

We now investigate the symmetry properties of the configurational Hamiltonian

$$\mathcal{H}^{\text{conf}}(J_1, J_2, \{n_{\mathbf{r}}\}) = \frac{1}{2}\sum_{h,k,l=1}^{2\ell} n_{hkl}\left(J_1 \sum_{h'k'l'} n_{h'k'l'} + J_2 \sum_{h''k''l''} n_{h''k''l''}\right) \tag{18}$$

under the transformation $J_1 \mapsto -J_1$. This qualitative analysis will shed light on the properties of the "liquid phase" derived from our model Hamiltonian as well as the interplay of long-range and short-range orders.

It is clear that the Hamiltonian has "sublattice symmetry:"[30] it is invariant under any transformations that swap interstitial sites and lattice sites, *i.e.* mappings such as $(hkl) \mapsto (h+1kl)$, $(hkl) \mapsto (hk+1l)$, $(hkl) \mapsto (hkl+1)$. If a configuration $\{n_{\mathbf{r}}\}$ preserves this symmetry, that is,

$$\sum_{(-1)^{h+k+l}=1} n_{hkl} = \sum_{(-1)^{h'+k'+l'}=1} n_{h'k'l'} = \frac{N}{2}; \tag{19}$$

then it is easy to find that

$$\mathcal{H}^{\text{conf}}(J_1, J_2, \{n_{\mathbf{r}}^*\}) = \mathcal{H}^{\text{conf}}(-J_1, J_2, \{n_{\mathbf{r}}\}) + 3NJ_1, \tag{20}$$

where its dual configuration $\{n_{\mathbf{r}}^*\}$ satisfies

TABLE I. In this table, all the elements (Ne, Ar, Kr, Xe, and Rn from the 0 group; Cu, Ag, and Au from the IB group) assume fcc structures in the solid phase (Ref. 29). T_E is the equilibrium melting point of crystals with surfaces. T_b is the boiling point of the liquid. ΔH_{vap} is the heat of evaporation. ΔH_{fus} is the heat of fusion. The data in the other rows are obtained or estimated as follows: $\Delta S_{\text{fus}}=\Delta H_{\text{fus}}/T_E$ is the entropy change due to fusion; $T_m=1.2T_E$ is an estimate of superheating limit based on Ref. 5; $|J_2|=(\Delta H_{\text{vap}}+\Delta H_{\text{fus}})/6N_A$ is a rough estimate for the J_2 parameter, where N_A is Avogadro's number.

	Ne	Ar	Kr	Xe	Rn	Cu	Ag	Au
T_E (K)	24.56	83.8	115.79	161.4	202	1357.6	1234.93	1337.33
T_b (K)	27.07	87.3	119.93	165.1	211.3	2840	2435	3129
ΔH_{vap} (kJ mol^{-1})	1.7326	6.447	9.029	12.636	16.4	300.3	250.58	334.4
ΔH_{fus} (kJ mol^{-1})	0.3317	1.188	1.638	2.297	2.89	13.05	11.3	12.55
ΔS_{fus} (J mol^{-1} K^{-1})	13.5	14.2	14.1	14.2	14.3	9.61	9.15	9.38
$\lvert J_2\rvert N_A$ (kJ mol^{-1})	0.3441	1.273	1.778	2.489	3.215	52.23	43.65	57.83
$9\lvert J_2\rvert/4k_B$ (K)	93.109	344.37	481.13	673.58	870.07	14134	11812	15649
T_m (K)	29.47	100.6	138.9	193.7	242.4	1629	1482	1604

$$2n^*_{hkl}-1=(-1)^{h+k+l}(2n_{hkl}-1). \tag{21}$$

Suppose there exists a temperature $T'\geqslant 0$ K, above which both the (J_1,J_2) and $(-J_1,J_2)$ systems are characterized by equal amounts of atoms occupying the lattice sites and interstitial sites. It follows that when $T>T'$, the dominant configurations in the partition functions for both cases should preserve the sublattice symmetry. From the obvious identity

$$\sum_{\{n_{\mathbf{r}}\}} e^{-\mathcal{H}^{\text{conf}}(J_1,J_2,\{n_{\mathbf{r}}\})/k_BT}=\sum_{\{n^*_{\mathbf{r}}\}} e^{-\mathcal{H}^{\text{conf}}(J_1,J_2,\{n^*_{\mathbf{r}}\})/k_BT}, \tag{22}$$

we see that when $T>T'$, the configurational free energy has the following correspondence:

$$F^{\text{conf}}(J_1,J_2,T)=F^{\text{conf}}(-J_1,J_2,T)+3NJ_1. \tag{23}$$

By differentiating with respect to T, we can establish the exact identity for configurational entropy:

$$S^{\text{conf}}(J_1,J_2,T)=S^{\text{conf}}(-J_1,J_2,T), \tag{24}$$

which holds for $T>T'$. This identity is definitely not true when temperature is sufficiently low, so that J_1 and $-J_1$ should result in different energy costs in excitation of interstitial defects, and the configurational entropy of the (J_1,J_2) and $(-J_1,J_2)$ systems would not be identical. Therefore, there must exist an intermediate temperature, at which $S^{\text{conf}}(J_1,J_2,T)-S^{\text{conf}}(-J_1,J_2,T)$ changes from a nonvanishing value to zero, suggesting the existence of a phase transition that enables the system to restore the sublattice symmetry.

The insensitivity of the configurational entropy with respect to the sign flip of J_1 is reminiscent of the "lattice gas model"[31] which describes the liquid phase in terms of the NNN attractive bonding energy, regardless of the nature of repulsion at NN distance. Therefore, the high-temperature solution of our model should correspond to a "liquid phase," where sublattice symmetry is preserved and accordingly, long-range order is lost: $\langle 2n_{\mathbf{r}}-1\rangle=0$. In the "liquid phase," $\langle n_{\mathbf{r}}n_{\mathbf{r}''}\rangle\approx\langle n_{\mathbf{r}}\rangle\langle n_{\mathbf{r}''}\rangle\equiv 1/4$ is definitely a bad approximation which rules out the temperature dependence of the ensemble average NNN occupancy $\langle n_{\mathbf{r}}n_{\mathbf{r}''}\rangle$, because the NNN correlation persists, keeping some short-range order even in the absence of long-range order. The persistent NNN correlation also constitutes a reason why we should evaluate the NNN average $\langle n_{\mathbf{r}}n_{\mathbf{r}''}\rangle$ more carefully than its NN counterpart, by taking into account the corrections proportional to $[1-L^2(\mathbf{r})]^2$.

B. The Poisson equation and a "chemical equilibrium" analog

By regarding the steady solid phase as a system reaching "chemical equilibrium," we may reaffirm the form of $\rho(L(\mathbf{r}))$ in the Poisson equation [Eq. (11)]. By probing into the dynamic process that leads to the chemical equilibrium, we may better understand why at a critical temperature, the equilibrium state in the context of a canonical ensemble is not attainable.

First, for $T<T_m$, we find that $\rho(L_T)=0$ is equivalent to the "chemical equilibrium" condition

$$\frac{1-|L_T|}{1+|L_T|}=\frac{[\text{defective cell}]}{[\text{nondefective cell}]}=e^{-\Delta\bar{\varepsilon}/k_BT}. \tag{25}$$

Here, $[\cdot]$ denotes the equilibrium concentration, and

$$\Delta\bar{\varepsilon}=2(\mathcal{H}_1-3k_BT\Upsilon)|L_T|-4\mathcal{H}_2|L_T|(|L_T|^2-1) \tag{26}$$

denotes the energy difference between two types of crystal cells: the *defective cell* incorporating (in the statistical parlance) more than one (inclusive) interstitial and the *nondefective cell* including less than one interstitial [visualized in the inset of Fig. 3(a)]. The terms related to J_1 and J_2 in the representation of $\Delta\bar{\varepsilon}$ could be recovered by the following "graph counting" process [in the graphs: $(1+|L_T|)/2=P$ and $(1-|L_T|)/2=q$]:

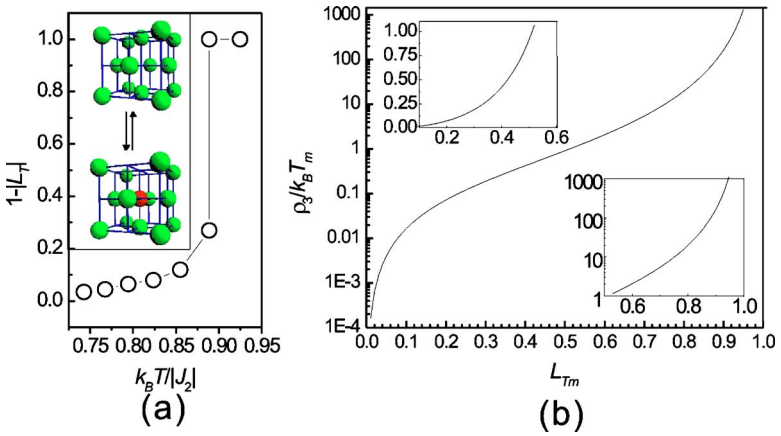

FIG. 3. (Color online) (a) L_T-T dependence for the same $\mathcal{H}_1/|\mathcal{H}_2|$ and Υ as in Fig. 2, where catastrophe occurs at the "melting point" $T_m = 0.89|J_2|/k_B$. Inset shows a "chemical equilibrium" between nondefective (up) and defective (down) cells at $T < T_m$. (b) The dimensionless parameter $\rho_3/k_B T_m$ as a function of L_{T_m} (inset shows close-ups with different scales). ρ_3 appears in the expression for $\pi\xi$, the critical size of the liquid nucleus.

$$-\frac{\Delta\bar{\varepsilon}}{4} = \frac{1}{4}\left(\bar{\varepsilon}_{\text{nondefective cell}} - \bar{\varepsilon}_{\text{defective cell}}\right) = \varepsilon_1 + \varepsilon_2, \quad (27)$$

$$\varepsilon_1 = \left(\begin{array}{c}\\ \end{array}\right) - \left(\begin{array}{c}\\ \end{array}\right)$$

$$= \left[3\left(\begin{array}{c}\\ \end{array}\right) + 3\left(\begin{array}{c}\\ \end{array}\right)\right.$$

$$+6\left(\begin{array}{c}\\ \end{array}\right) + 3\left(\begin{array}{c}\\ \end{array}\right)$$

$$\left.+3\left(\begin{array}{c}\\ \end{array}\right)\right] - \left[3\left(\begin{array}{c}\\ \end{array}\right)\right.$$

$$+3\left(\begin{array}{c}\\ \end{array}\right) + 6\left(\begin{array}{c}\\ \end{array}\right)$$

$$\left.+3\left(\begin{array}{c}\\ \end{array}\right) + 3\left(\begin{array}{c}\\ \end{array}\right)\right]$$

$$= \left(3\frac{J_1}{4}q + 3\frac{J_2}{2}P + 6\frac{J_1}{4}qP + 3\frac{J_2}{2}q^2 + 3\frac{J_2}{2}P^2\right)$$

$$-\left(3\frac{J_1}{4}P + 3\frac{J_2}{2}q + 6\frac{J_1}{4}Pq + 3\frac{J_2}{2}P^2 + 3\frac{J_2}{2}q^2\right)$$

$$= \frac{3}{4}(-J_1 + 2J_2)(P - q) = \frac{3}{4}(-J_1 + 2J_2)|L_T|, \quad (28)$$

$$\varepsilon_2 = \left[\left(\begin{array}{c}\\ \end{array}\right) - 3\left(\begin{array}{c}\\ \end{array}\right)\right]$$

$$-\left[\left(\begin{array}{c}\\ \end{array}\right) - 3\left(\begin{array}{c}\\ \end{array}\right)\right]$$

$$= \left(\frac{3J_2}{2}P^3 - 3\frac{J_2}{2}P^2\right) - \left(\frac{3J_2}{2}q^3 - 3\frac{J_2}{2}q^2\right)$$

$$= -\frac{3J_2}{2}(P - q)Pq = \frac{3J_2}{8}|L_T|\left(|L_T|^2 - 1\right). \quad (29)$$

In this counting, the probability that an atom occupies a site is labeled at the corresponding vertex. ε_1 evaluates the energy difference between two types of cells regardless of the cooperativity of (i.e., correlation between) NNN atoms; ε_2 considers the energy offset due to the tendency for simultaneous occupation or evacuation of the three sites that are NNN to the probability-1-occupied site.

This dynamical equilibrium is achieved by stochastic creation and annihilation of interstitial defects, or more vividly speaking, the collisions in a dilute "gas" of interstitial monomers and interstitial oligomers, in search of a minimal free energy corresponding to an optimized long-range order parameter L_T [Fig. 3(a)].

Second, we notice that the aforementioned "collision process" causes a fluctuation of $L(\mathbf{r})$, governed by Eq. (11) which resembles the equation for a globally neutral plasma when $T \ll T_m$. [This is because $\rho(L(\mathbf{r}))$ changes sign as $L(\mathbf{r})$ varies in the vicinity of L_T, which is analogous to the coexistence of positive and negative charges in a plasma.] The Green's function of fluctuation response $G(\mathbf{r}, \mathbf{r}^{\#})$ satisfies

$$\frac{2^{3/2}}{a^3}\left[\gamma\nabla^2 + \frac{\partial\rho(L(\mathbf{r}))}{\partial L(\mathbf{r})}\right]G(\mathbf{r}, \mathbf{r}^{\#}) = -k_B T\delta(\mathbf{r} - \mathbf{r}^{\#}), \quad (30)$$

where $\delta(\mathbf{r} - \mathbf{r}^{\#})$ is the Dirac delta function. For sufficiently low temperature $T < T_m$, the partial derivative in the equa-

tionabove is negative, so $G(\mathbf{r},\mathbf{r}^{\#})$ is a propagator that decays exponentially as $|\mathbf{R}|=|\mathbf{r}-\mathbf{r}^{\#}|$ grows. This guarantees the stability of the homogeneous distribution $L(\mathbf{r})\equiv L_T$ and implies that there is no global net flow of particles in the solid, which is the hallmark of the canonical ensemble. However, as T approaches T_m from below, it is possible that $\partial\rho(L(\mathbf{r}))/\partial L(\mathbf{r})>0$ for certain values of $L(\mathbf{r})$ not far from L_T, which results from a non-Gaussian perturbation to the homogeneous distribution. When $T=T_m$, which is defined in Eq. (12), the "phenomenological electric charge density" $\rho(L(\mathbf{r}))$ no longer changes its sign in the vicinity of L_{T_m}, and could be expanded as $\rho(L(\mathbf{r}))=-\mu^2(\mathbf{r})\rho_2-\mu^3(\mathbf{r})\rho_3+\cdots$ in the vicinity of L_{T_m}, where $\mu(\mathbf{r})=L(\mathbf{r})-L_{T_m}$. At this critical temperature, the fluctuation is governed by $\gamma\nabla^2\mu(\mathbf{r})=\mu^2(\mathbf{r})\rho_2+\mu^3(\mathbf{r})\rho_3$. As $r\to 0$, this equation gives $\mu(\mathbf{r})\sim-\rho_2/\rho_3\neq 0$ for the isotropic perturbation and $\mu(\mathbf{r})\propto r^l Y_{lm}(\theta,\phi)$ for all anisotropic perturbations where $l>0$. Therefore, isotropic excitation dominates the instability mechanism at T_m, because all the Y_{lm} $(l>0)$ modes are overwhelmed by the Y_{00} mode in the short range.

Furthermore, $\mu(\mathbf{K})$ the Fourier transform of $\mu(\mathbf{r})$, has the following behavior (V being the volume of the system):

$$\begin{aligned}\langle|\mu(\mathbf{K})|^2\rangle &\equiv \int |\mu(\mathbf{K})|^2 e^{-F/k_BT_m}\prod_{\mathbf{K}} d\mu(\mathbf{K}) \Bigg/ \int e^{-F/k_BT_m}\prod_{\mathbf{K}} d\mu(\mathbf{K}) \\ &\approx \frac{k_BT_m\gamma K^2}{V}\left[\gamma^2K^4-\frac{1}{4}\frac{\rho_3 k_BT_m}{\pi^2\xi^3}c(c^2+3)+O\left(\frac{1}{K^2}\right)\right]^{-1},\end{aligned} \tag{31}$$

where $c\xi^{-1}$ is the spectral width, that is, the $\mathbf{K}$'s satisfying $(1-c)\xi^{-1}<|\mathbf{K}|<(1+c)\xi^{-1}$ dominate the following sums over wave vectors:

$$\begin{aligned}F[L(\mathbf{r})]-F[L_{T_m}] &= V\sum_{\mathbf{K}}\frac{\gamma}{2}K^2|\mu(\mathbf{K})|^2+\frac{V\rho_2}{3}\sum_{\mathbf{K}_1+\mathbf{K}_2+\mathbf{K}_3=\mathbf{0}}\mu(\mathbf{K}_1)\mu(\mathbf{K}_2)\mu(\mathbf{K}_3) \\ &\quad+\frac{V\rho_3}{4}\sum_{\mathbf{K}_1+\mathbf{K}_2+\mathbf{K}_3+\mathbf{K}_4=\mathbf{0}}\mu(\mathbf{K}_1)\mu(\mathbf{K}_2)\mu(\mathbf{K}_3)\mu(\mathbf{K}_4)+\cdots.\end{aligned} \tag{32}$$

Viewing $\langle|\mu(\mathbf{K})|^2\rangle$ as a complex-valued function of the complex wave number K, and leaving alone the $O(K^{-2})$ term, we see that $\langle|\mu(\mathbf{K})|^2\rangle$ not only has poles at purely imaginary K values (decay mode), but also encounters singularities at real-valued K's (oscillation mode), indicating that homogeneity is only preserved for a finite volume within which fluctuation propagates as a sinusoidal wave. The characteristic length of this wave $\xi=4\pi^2\gamma^2 2^{3/2}[\rho_3 k_BT_m c(c^2+3)a^3]^{-1}$ appears in the following estimate:

$$\begin{aligned}G(\mathbf{R}) &= \frac{V}{(2\pi)^3}\int d^3\mathbf{K}\langle|\mu(\mathbf{K})|^2\rangle e^{i\mathbf{K}\cdot\mathbf{R}} \\ &\approx \frac{k_BT_m}{8\pi\gamma R}\left(e^{-R/\xi}+\cos\frac{R}{\xi}\right).\end{aligned} \tag{33}$$

The sinusoidal propagator at $T=T_m$ facilitates particle exchange throughout the solid, thereby declaring the end of the superheating process[8] and demise for the grand canonical ensemble. In this context, "quasineutrality" in the "plasma" is attained by establishing $L(\mathbf{r})>0$ and $L(\mathbf{r})<0$ domains, each with diameter of $\pi\xi\sim\sqrt{2}a\mathcal{H}_1^2\pi^3(2\rho_3k_BT_m)^{-1}$, which is the average size of the locally isotropic excitations of atom clusters.[33] [Fig. 3(b) plots the dimensionless parameter $\rho_3/k_BT_m=8\lambda^{-3}\int_0^\lambda x^4(1-x^2)^{-4}dx$, where $\lambda=L_{T_m}$.[32]]

These highly cooperative and energetic atom clusters give rise to a catastrophe of global long-range order at T_m:

$$|L_T|\begin{cases}\to|L_{T_m}|\neq 0, & T\to T_m-0, \\ =0, & T>T_m.\end{cases} \tag{34}$$

The vanishing long-range order $|L_T|$ at temperatures higher than T_m casts the system into sublattice symmetry.

C. Relations with Born and Lindemann criteria: "Lindemann particle clusters" reconsidered

Within the spherical domains of instability (SDIs) described above as locally isotropic excitations, due to the nature of the fluctuation and the relaxation, the displaced atoms are moving collaboratively, energetically and isotropically, in many ways similar to "Lindemann particles."[5] Regarding these characteristics of SDIs, we can obtain three results after restoring the lattice distortions into our model. First, the totality of atoms in each SDI exhibits local isotropy, which guarantees exactly vanishing shear modulus difference:

$$\Delta C_S = C_{44}-\frac{C_{11}-C_{12}}{2}=0. \tag{35}$$

Second, the average displacement of the energetic atoms in all the SDIs exceeds $a\delta_L^*$, the average displacement of all atoms, because packed spherical domains cannot perfectly fill the whole space. In the light of this, the atoms in SDIs are "Lindemann particles" by definition. Third, the critical Lindemann ratio δ_L^* is determined by the solving the Langevin equation $m\overline{\mathbf{r}(t)\cdot\ddot{\mathbf{r}}(t)}=\overline{\mathbf{r}(t)\cdot\mathbf{F}(t)}$. Here, m is the mass of the atom, on which a force $\mathbf{F}(t)$ is exerted at time t. The overbar indicates the time average. According to the ergodicity argument, we may replace the time average by the ensemble average as long as $T<T_m$, and then take the limit $T\to T_m-0$ to conclude that

$$3k_BT_m=4\pi^2\langle\nu^2\rangle m(a\delta_L^*)^2 \tag{36}$$

where $\langle\nu^2\rangle$ is the average square frequency.[3]

IV. DISCUSSIONS

In short, the aforementioned SDIs satisfy the Born and Lindemann instabilities simultaneously and make the avalanche of atom displacement and the rigidity catastrophe coincide. In addition to providing the mechanism (*why*) and pathway (*how*) of melting and bridging the Born and Lindemann criteria in a fcc elemental crystal (Ar, Cu, etc.), our account of the SDIs is capable of answering the three questions about SLPT intractable by numerical simulation. (1)

The most influential factors for the critical Lindemann ratio δ_L^* are the profile (not every detail) of the interatomic force that determines $\langle L\rangle_{T_m}$ as a function of J_1, J_2, and Υ in different crystals. Although it might be true that $m\langle\nu^2\rangle \propto |\mathcal{H}_2| \propto T_m$ for the Lennard-Jones potential that govern interactions of noble gas molecules (Table I), and there is a universal dimensionless parameter δ_L^* for all van der Waals crystals with fcc geometry, there is not necessarily a general δ_L^* applicable to all fcc crystals.[7] (2) The residual shear modulus at T_m is due to the fact that there is always some unoccupied space among the packed spheres. Born's argument is still valid within each SDI, but no longer valid in the melting crystal as a whole. (3) Inhomogeneous instability comes from fluctuations that propagate as a sinusoidal wave, which is a consequence of the optimization of the free-energy functional in the thermodynamic limit. Although this wave cuts the space into separate compartments exhibiting ostentatiously mutual independence, it actually gives rise to huge density fluctuations throughout the solid and facilitates the exchange of particles between different sites in the space, thus declaring the demise of canonical ensemble. Hence, this wave digs out channels for particle flow in addition to energy flow within the solid phase, thereby putting an end to the superheating process.[8] This reaffirms the numerical conclusions in Ref. 5 that the Lindemann particles in the "surface-free melting" process have the same function as the surface boundaries in "surface melting:" they both form an outlet for particle exchange, the key machinery in "melting" problems.

V. CONCLUSIONS

In this paper, we have studied the surface-free fcc crystal with a dynamic lattice gas J_1-J_2 model. The mean-field approximation solution shows that the long-range order catastrophe is triggered by the correlation of interstitial defects near T_m, which leads to a heterogeneous formation of instability nuclei. Since the preliquid droplets satisfy the Born and Lindemann criteria simultaneously, these nuclei facilitate particle flow as do surface boundaries in surface melting. The most striking result is that the nucleation process within the scope of this minimal model not only reconciles two melting criteria, but also serves as a bridge that joins two ensemble theories: the canonical and the grand canonical. This shows evidence that the driving force of melting may come from the interior of the solid phase itself.

ACKNOWLEDGMENTS

This work is supported by the National Natural Science Foundation of China and the 973 Project of the Science and Technology Ministry of China, and Shanghai Science and Technology Committee.

*Present Address: Department of Chemistry and Chemical Biology, Harvard University, Cambridge, MA 02138.

†Author to whom correspondence should be addressed. Email address: xfjin@fudan.ac.cn

[1] R. W. Cahn, Nature (London) **273**, 491 (1978); **323**, 668 (1986).

[2] J. G. Dash, Rev. Mod. Phys. **71**, 1737 (1999).

[3] F. A. Lindemann, Phys. Z. **11**, 609 (1910); J. J. Gilvarry, Phys. Rev. **102**, 308 (1956).

[4] M. Born, J. Chem. Phys. **7**, 591 (1939).

[5] Z. H. Jin, P. Gumbsch, K. Lu, and E. Ma, Phys. Rev. Lett. **87**, 055703 (2001).

[6] J. L. Tallon, Philos. Mag. A **39**, 151 (1978).

[7] G. Grimvall and S. Sjodin, Phys. Scr. **10**, 340 (1974).

[8] K. Huang, *Statistical Mechanics*, 2nd ed. (John Wiley and Sons, New York, 1987).

[9] B. Rethfeld, K. Sokolowski-Tinten, and D. von der Linde, Phys. Rev. B **65**, 092103 (2002).

[10] A. Trayanov and E. Tosatti, Phys. Rev. B **38**, 6961 (1988); R. Ohnesorge, H. Löwen, and H. Wagner, Phys. Rev. E **50**, 4801 (1994); J. Q. Broughton and G. H. Gilmer, J. Chem. Phys. **79**, 5095 (1983); **79**, 5105 (1983).

[11] F. H. Stillinger and T. A. Weber, J. Chem. Phys. **81**, 5095 (1984).

[12] J. Cardy, J. Phys. A **29**, 1897 (1996).

[13] A. V. Granato, Phys. Rev. Lett. **68**, 974 (1992).

[14] M. I. Baskes, Phys. Rev. Lett. **83**, 2592 (1999).

[15] V. Halpern, J. Phys.: Condens. Matter **12**, 4303 (2000).

[16] N. Sandberg, B. Magyari-Köpe, and T. R. Mattsson, Phys. Rev. Lett. **89**, 065901 (2002).

[17] K. Nordlund and R. S. Averback, Phys. Rev. Lett. **80**, 4201 (1998).

[18] A. Bongiorno, L. Colombo, F. Cargnoni, C. Gatti, and M. Rosati, Europhys. Lett. **50**, 608 (2000).

[19] S. Birner, J. P. Goss, R. Jones, P. R. Briddon, and S. Öberg, in Proceedings of ENDEASD, Stockholm, 2000, http://newton.ex.ac.uk/research/qsystems/jones/papers/latest/ENDEASD/Stockholm_Birner.pdf.

[20] J. I. Landman, C. G. Morgan, J. T. Schick, P. Papoulias, and A. Kumar, Phys. Rev. B **55**, 15 581 (1997).

[21] K. W. Ingle, R. C. Perrin, and H. R. Schober, J. Phys. F: Met. Phys. **11**, 1161 (1981).

[22] L. Salter, Proc. R. Soc. London, Ser. A **233**, 418 (1956); L. Dobrzynski and J. Friedel, Surf. Sci. **12**, 649 (1968); G. Allan and M. Lannoo, in *Defects and Radiation Effects in Semiconductors*, edited by R. R. Hasiyuti (Institute of Physics, Bristol, 1980).

[23] L. D. Landau and E. M. Lifshitz, *Statistical Mechanics, Part I* (Butterworth-Heinemann, London, 1999).

[24] V. L. Ginzburg, Sov. Phys. Solid State **2**, 1824 (1960).

[25] A. Onuki, *Phase Transition Dynamics* (Cambridge University Press, Cambridge, U.K., 2002).

[26] The total free-energy functional $F[L(\mathbf{r})]=F^{\mathrm{vib}}[L(\mathbf{r})]+F^{\mathrm{conf}}[L(\mathbf{r})]$ is invariant under the transformation $L(\mathbf{r})\mapsto -L(\mathbf{r})$ for all $\mathbf{r}$, as required by the equivalent status of Na-like and Cl-like sublattices at all temperatures. Accordingly, $\rho(-L(\mathbf{r}))=-\rho(L(\mathbf{r}))$. At sufficiently low temperatures, however, the energy cost to flip the sign of $L(\mathbf{r})$ for all sites is too high, so the configurations that the system can sample through at most account for *half* of all possible ways to arrange N atoms on $2N$ sites. This is an example of "sublattice symmetry breaking" (see also Sec. III A

and Ref. 30). Two nonzero roots of $\rho(\lambda)=0$, say, $\lambda=\pm|L_T|$, both minimize the free energy at a sufficiently low temperature T.

[27] J. D. Jackson, *Classical Electrodynamics*, 3rd ed. (Wiley Textbooks, New York, 1998).

[28] The first-order phase transition here is not associated with a cubic term in the expansion of the Hamiltonian, but an interplay of logarithmic, quadratic, and fourth-power terms of $L(\mathbf{r})$. A similar argument exists for the first-order phase transition in weak itinerant ferromagnets at low temperatures, as shown by D. Belitz, T. R. Kirkpatrick, and Thomas Vojta, Phys. Rev. Lett. **82**, 4707 (1999).

[29] The first four rows were taken from the descriptions of individual elements in the online encyclopedia http://en.wikipedia.org/

[30] N. Goldenfeld, *Lectures on Phase Transitions and the Renormalization Group* (Addison-Wesley, Reading, MA, 1992).

[31] C. N. Yang and T. D. Lee, Phys. Rev. **87**, 404 (1957); T. D. Lee and C. N. Yang, *ibid.* **87**, 410 (1957).

[32] From the expression $\rho_3(L_{T_m})$, it is evident that $\rho_3\to 0$ and $\pi\xi\to\infty$ in the limit $L_{T_m}\to 0$. This reinforces the previous argument that $L_{T_m}=0$ corresponds to a continuous phase transition in terms of an infinite correlation length.

[33] For the case shown in Fig. 2, $\pi\xi\sim 15.03a$, and the spherical volume $\pi(\pi\xi)^3/6\sim 1780a^3$ forms a good comparison with the statement in Ref. 5 that the "Lindemann particle" clusters consist of 10^2–10^3 atoms.